JOURNAL OF PROTEOMICS 75 (2012) 1778–1791

Available online at www.sciencedirect.com

SciVerse ScienceDirect

www.elsevier.com/locate/jprot

Increased expression and phosphorylation of the two S100A9 isoforms in mononuclear cells from patients with systemic lupus erythematosus: A proteomic signature for circulating low-density granulocytes

Esther J. Pavón[a,1], *Sonia García-Rodríguez*[a], *Esther Zumaquero*[a,2], *Rubén Perandrés-López*[a], *Antonio Rosal-Vela*[a], *Antonio Lario*[b], *Victoria Longobardo*[b], *Montserrat Carrascal*[c], *Joaquín Abián*[c], *José-Luis Callejas-Rubio*[d], *Norberto Ortego-Centeno*[d], *Mercedes Zubiaur*[a], *Jaime Sancho*[a,*]

[a]*Departamento de Biología Celular e Inmunología, Instituto de Parasitología y Biomedicina "López-Neyra", IPBLN-CSIC, Armilla, Spain*
[b]*Unidad de Proteómica, Instituto de Parasitología y Biomedicina "López-Neyra", CSIC, Armilla, Spain*
[c]*CSIC/UAB Proteomics Laboratory, Instituto de Investigaciones Biomédicas de Barcelona-Consejo Superior de Investigaciones Científicas (IIBB-CSIC/IDIBAPS), Building M, Barcelona Autonomous University, E-08193 Bellaterra, Spain*
[d]*Unidad de Enfermedades Autoinmunes Sistémicas, Hospital Universitario San Cecilio, Granada, Spain*

ARTICLE INFO

Article history:
Received 19 July 2011
Accepted 14 December 2011
Available online 30 December 2011

Keywords:
Low-density granulocytes
Lupus
Phosphorylation
PTMs
S100A9

ABSTRACT

Proteins differentially expressed in peripheral blood mononuclear cells (PBMCs) from systemic lupus erythematosus (SLE) patients versus Normal controls were identified by 2-DE and MALDI-MS. Thus, S100A9 expression was significantly increased in SLE PBMCs relative to Normal PBMCs at both mRNA and protein levels. Increased S100A9 levels in SLE PBMCs correlated positively with the abnormal presence of low-density granulocytes (LDGs) detected by flow-cytometry in the mononuclear cell fractions. Another set of proteins that were differentially expressed in SLE PBMCs formed S100A9-independent clusters, suggesting that these differences in protein expression are in fact reflecting changes in the abundance of specific cell types. In SLE PBMCs spots of the two S100A9 isoforms, S100A9-l and S100A9-s, and their phosphorylated counterparts were identified and confirmed to be phosphorylated at Thr^{113} by MS/MS analyses. In addition, the phorbol ester PMA alone or in combination with ionomycin induced a stronger increase in threonine phosphorylation of S100A9 in SLE than in Normal PBMCs, while the same stimuli caused the opposite effect on phosphorylation and activation of Erk1/2, suggesting the existence of an abnormal S100A9 signaling in SLE PBMCs. Therefore, the expansion and activation of LDGs in SLE seems to underlie this prominent S100A9 signature.

* *Corresponding author at:* IPBLN-CSIC, Parque Tecnológico de Ciencias de la Salud, Avenida del Conocimiento s/n, 18100 Armilla (Granada), Spain. Fax: +34 958 181632.
E-mail address: granada@ipb.csic.es (J. Sancho).
[1] New Address: Hospital Universitario San Cecilio, Ciber de Enfermedades Hepáticas y Digestivas (CIBEREHD), Granada, Spain.
[2] New Address: University of Rochester Medical Center, Rochester, USA.

1874-3919/$ – see front matter
doi:10.1016/j.jprot.2011.12.020

1. Introduction

SLE is a systemic autoimmune disease characterized by a waxing and waning course and the involvement of multiple organs, including skin, kidneys, and central nervous system [1]. SLE patients display multiple abnormalities in T cell antigen-mediated signaling that lead to B cell hyper-responsiveness, increased apoptosis, skewed cytokine production, and breakdown of immunological tolerance (reviewed in [2], and [3]). Although SLE ethiopathology is poorly understood, there is likely a role for environmental triggers, for instance viruses, acting in the context of susceptibility genes [4,5].

Increased serum levels of the S100A8/A9 heterodimer, calprotectin, in SLE was first described by Kuruto et al. [6], and it has been later confirmed by other groups [7–9]. The latter group has also found increased levels of S100A9/A8 heterodimer on the surface of many SLE cell types [9], which could be linked to the release of neutrophils extracellular traps containing calprotectin [10]. Regarding differential expression of S100A9, S100A8, or S100A8/A9 in distinct cell types in SLE patients, Frosch et al., [11] demonstrated that different forms of glomerulonephritis (GN), including SLE GN, were associated with the appearance of certain phenotypes of infiltrating macrophages characterized by expression of S100A8 and S100A9 as well as by their S100A8/A9 complex formation. Increased expression of S100A8 and S100A9 was restricted to the sites of active inflammation. On the other hand, Dai, Y., et al., detected increased S100A9 protein expression in SLE PBMCs [12], without further description of which cell subset was in fact expressing this protein. Expression of S100A8 and S100A9 is up-regulated in epidermal cells from mice with cutaneous lupus erythematosus [13], and stimulation of $CD8^+$ T cells from humans with lupus erythematosus with S100A9 or S100A8 proteins results in substantial upregulation of IL-17 expression via TLR4 ligation, suggesting a key role for these proteins for the development of autoreactive lymphocytes during human autoimmunity as well [13].

PBMCs are composed of immune cells from either the innate immune system (NK cells) or the adaptive immune system (T and B lymphocytes) or both (monocytes and DCs). Therefore, a proteomic analysis of these cells may help to identify etiopathogenic factors and predictors of disease activity. Thus, differences in expression of several PBMC proteins have been observed between clinically active and inactive SLE patients by using iTRAQ labeled SLE PBMCs [14]. However, most of these proteomic studies do not assign the identified proteins to a specific cell subset or blood constituent [15]. In the present study proteins differentially expressed in PBMCs from SLE patients and healthy control subjects were identified by 2-DE and MALDI-TOF MS. The data show that mononuclear cells from SLE patients overexpress phosphorylated S100A9 isoforms, which constitute a proteomic signature of the presence of increased number of circulating low-density granulocytes.

2. Materials and methods

2.1. Patients and healthy controls

Fourty four outpatients fulfilling the revised American College of Rheumatology (ACR) criteria for the diagnosis of SLE [16], and routinely followed in the Systemic Autoimmune Diseases Unit (Hospital Clínico San Cecilio, Granada, Spain) participated in this study. Thirty six healthy, age-matched volunteers served as controls. Because the paucity of cell numbers obtained from the disease group, some of them were leukopenic, different sets of experiments were performed with different patient groups: 1) *Differential protein expression by 2-DE*. In the differential protein expression study, samples from 14 SLE patients and 15 Normal controls were analyzed. 2) *Validation by Western blotting*. To validate the differential expression data, samples from 30 SLE patients and 30 Normal controls were analyzed. The SLE group included samples from 12 SLE subjects that were first analyzed by 2-DE, and samples from 18 additional subjects that were analyzed for the first time. The Normal control group included 9 samples from subjects that were first analyzed by 2-DE, and 21 additional samples from subjects that were analyzed for the first time. 3) *Validation by real-time RT-PCR*. Samples from 14 SLE subjects who had not been analyzed by 2-DE, nor by Western-blotting were used. As shown in supplemental Table 1, there were not major differences in clinical or demographic characteristics of these three SLE groups. Disease activity was scored and the SLE Disease Activity Index (SLEDAI) was calculated [17]. All of them were Caucasians. Complete blood cell count, serum complement and serum anti-nuclear and anti-DNA antibodies were measured in all patients. The study protocol was approved by the Hospital Clínico San Cecilio, and CSIC Review Board and Ethics Committees. Written informed consent was obtained from all participating patients and volunteers according to the Declaration of Helsinki.

2.2. Purification of peripheral blood mononuclear cells (PBMC) and flow cytometry immunophenotyping

Blood was collected by the BD Vacutainer system into K_2-EDTA tubes (BD Diagnostics, NJ, USA) and PBMC were isolated by density gradient centrifugation over HISTOPAQUE®-1077 (Sigma–Aldrich Química, S.A., Spain) following manufacturer's instructions. The mononuclear fraction was resuspended in Hank's solution containing 2% Fetal Bovine Serum (FBS, GIBCO, Invitrogen), 2 mM EDTA and 20 mM HEPES pH 7.4 (Hank's-FBS). Remaining erythrocytes were lysed in a solution containing ammonium chloride (2–3 min), and then cells were washed twice (250 ×g, 10 min) in Hank's-FBS-EDTA. PBMC were analyzed for surface expression of CD3 (T cells), CD19 (B cells), CD56 (NK cells), or CD15 (granulocytes) by single or double-staining using FITC-, or PE-labeled anti-CD3, anti-CD19, anti-CD56, and anti-CD15 mAbs in the relevant combinations. Compensation settings were adjusted using single stained PBMC samples. Isotype-matching labeled antibodies were used to calculate the nonspecific staining. Lymphocytes, monocytes, and granulocytes were gated according with their forward and scatter characteristics as described [18]. Two color immunofluorescence analyses were performed on a FACScan flow cytometer (BD Biosciences, San Jose, CA), using the CellQuest Pro (BD Biosciences), and FlowJo (Tree Star, Inc. San Carlos, CA) software.

2.3. Two-dimensional gel electrophoresis

PBMCs were washed with a Hank's solution FBS-free before protein extraction. Then, plasma membrane and cytosolic proteins

were extracted from PBMCs NP-40 lysates upon separation from intact nuclei and NP-40-insoluble material as described [19]. Proteins were precipitated with methanol/chloroform [20] and pellet was solubilized in ReadyPrep 2-D Rehydration/Sample Buffer 1: 7 M urea, 2 M thiourea, 1% (w/v) ASB-14, 40 mM Tris base, 2 mM tributylphosphine (TBP), 0.2% (w/v) Bio-Lyte 3/10 ampholytes, and 0.001% Bromophenol Blue (Bio-Rad). 2-DE was carried out using the Protean IEF cell and Criterion electrophoresis cell systems (Bio-Rad. Hercules, CA, USA) [21] with the following modifications. First-dimension IPG strips (Bio-Rad: 11 cm, linear pH 3–10 gradient, unless otherwise indicated) were loaded with the solubilized samples through passive in-gel rehydration 12–18 h at 20 °C. The 11 cm IPG strips were focused in a one-step procedure, at 8000 V for a total of 35,000 Vh at 20 °C with a current limit of 50 μA. Prior to the second-dimension separation, the focused strips were equilibrated for 10 min in Equilibration Buffer I (6 M urea, 2% SDS, 0.375 M Tris–HCl (pH 8.8), 20% glycerol, and 2% (w/v) DTT) followed by another 10 min in Equilibration Buffer II (Equilibration Buffer I with 2.5% (w/v) iodoacetamide instead of DTT). The equilibrated IPG strips were positioned on Criterion XT Precast Gels (4–12% gradient in XT MES buffer) and the separation was performed at 150 V at room temperature. The gels were fixed for 30 min in 10% methanol, 7% acetic acid and stained overnight with SYPRO Ruby fluorescent stain (Bio-Rad) according with manufacturer's instructions. The stained gels were scanned with a Typhoon 9400 system (Amersham Biosciences). Then gels were washed with ddH_2O and stained for 60 min with Bio-Safe stain (Bio-Rad) and scanned using a GS-800 Calibrated densitometer (Bio-Rad). Digitalized gel images were analyzed with the PDQuest software version 7.2 (Bio-Rad). The intensity of each spot in a gel was normalized as a proportion of the total protein intensity detected for the entire gel (relative volume).

2.4. *In-gel digestion of proteins*

Gel pieces containing the proteins of interest were manually excised and subjected to in-gel digestion with trypsin (Promega, Madison, WI) using a Digest MSPro (Intavis, Koeln, Germany) following standard procedures. Briefly, gel slices were washed once with 50 mM ammonium bicarbonate/50% ethanol followed by 100% ethanol, reduced with 10 mM DTT, alkylated with 55 mM iodoacetamide, washed twice with 50 mM BCA, dehydrated with acetonitrile and then digested with trypsin for 6 h at 37 °C. Peptides were extracted with 0.2% TFA. Volume was reduced to 10 μl in a Speed-Vac and passed through a $ZipTip_{\mu\text{-}C18}$ Pipette Tip (Millipore). Peptides were eluted with 60% acetonitrile/0.1% TFA.

2.5. *Protein identification by MALDI-TOF MS*

Proteins were identified by peptide mass fingerprinting (PMF) using a Voyager-DE PRO MALDI-TOF (AB SCIEX, CA) instrument in positive reflectron mode. For the analysis, 1 μL of the peptide extract and 1 μL of matrix (α-cyano-4-hydroxycinnamic acid, 5 mg/ml) were loaded in the MALDI plate and were let to dry. Spectra were internally calibrated using ions at 842.5 *m/z* and 2211.1 *m/z* derived from the trypsin autodigestion. Data Explorer 4.0 (Applied Biosystems) was used to create the "peak list".

2.6. *MALDI LIFT-TOF/TOF sequence analysis*

Sequence analyses were performed on an Ultraflex MALDI-TOF/TOF instrument (Bruker, Germany). Samples were prepared using α-cyano-4-hydroxy-cinnamic acid as a matrix on anchor chip targets (Bruker, Germany), as described by the manufacturer. The spectra and mass lists were exported to BioTools (Version 3.0, Bruker Daltonics) for database search and spectrum annotation.

2.7. *Database search*

The public MASCOT server (http://www.matrixscience.com/cgi, Matrix Science, London, UK) was used for protein identification from the peptide-mass fingerprint with the following parameters: peptide tolerance 50 ppm, enzyme set as trypsin and allowance up to one missed cleavages, fixed modification was cysteine carbamidomethylated (+57 Da) and variable modifications were methionine oxidation (+16 Da), N-terminal acetylation (+42 Da), and phosphorylation (+80 Da). The SwissProt database (version 2011_03, 20234 entries) was used for the search. The MSDB database (version 20070222, 3239079 sequences) was used for MS/MS data analysis.

2.8. *Calprotectin plasma levels*

Plasma calprotectin (S100A8/S100A9 heterocomplex) was measured using a commercial Enzyme Linked Immunosorbent Assay (ELISA) kit (Hycult Biotech, Uden, The Netherlands). All measurements were performed in duplicate according to the manufacturer's instructions. S100A8 and S100A9 form non-covalently associated complexes in the presence of calcium which are detected by the ELISA system used. The ELISA was therefore calibrated with the native S100A8/S100A9 complex and data expressed as ng/ml S100A8/S100A9. The sensitivity of the assay was 1.6 ng/ml.

2.9. *Stimulation of PBMCs*

PBMCs from SLE patients or Normal controls were resuspended in RPMI-Hepes at 10×10^6 cells/ml and incubated 10 min at 37 °C before adding Ionomycin at 200 ng/ml, or PMA at 400 ng/ml, or PMA (400 ng/ml) + Ionomycin (200 ng/ml), or medium and then incubated for 10 min at 37 °C as described [22]. Upon addition of 1 ml of ice-cold RPMI-Hepes cells were spun down at 4000 rpm and lysed in 1% NP-40 lysis buffer as described [19].

2.10. *Western blot analysis*

NP-40 PBMC lysates corresponding to 5×10^5 cell-equivalents were diluted in 3× Laemmli's sample buffer. Proteins were separated on 15% acrylamide SDS-PAGE under reducing conditions, transferred to PVDF membranes and immunoblotted as described [23]. The following primary polyclonal or monoclonal antibodies were from Santa Cruz Biotechnology (CA): Calgranulin A (FL-83) is a rabbit polyclonal antibody raised against amino acids 1–83 representing full length Calgranulin A of human origin; Calgranulin B (H-90) is a rabbit polyclonal antibody raised against amino acids 25–114 mapping at the

C-terminus of Calgranulin B of human origin; HSP90α/β (H-114) is a rabbit polyclonal antibody raised against amino acids 610–723 mapping at the C-terminus of HSP 90β of human origin, which recognizes both HSP 90α and HSP 90β; HSP70 (W-27) is a mouse monoclonal antibody raised against HSP 70 from HeLa cells; CypA (C-14)-R is a rabbit polyclonal antibody against human Cyclophilin A. Erk 2 (C-14) is a rabbit polyclonal antibody against a peptide mapping the C-terminus of rat Erk 2 that recognizes Erk 2 p42 and, to a lesser extent, Erk 1 p44 of several species, including human. The anti-phosphothereonine specific antibody was from Zymed (San Francisco, CA), and the the anti-Phospho-p44/42 MAPK (Erk1/2) (Thr^{202}/Tyr^{204}) antibody was from Cell Signaling (New England Biolabs, MA). The latter antibody detects endogenous levels of p44 and p42 MAP Kinase (Erk1 and Erk2) when phosphorylated either individually or dually at Thr^{202} and Tyr^{204} of Erk1 (Thr^{185} and Tyr^{187} of Erk2) as described [23]. The HRP-conjugates of the secondary antibodies: Goat Anti-Rabbit IgG (H+L), and Goat anti-Mouse IgG (H+L) were from Promega Corporation.

2.11. *RNA isolation and gene expression analyses by real-time RT-PCR*

Expression of genes mRNA was monitored using reverse transcription polymerase chain reaction (RT-PCR). Total RNA was isolated from PBMC pellets using RNeasy Plus mini kit (BD-Qiagen, Hilden, Germany) according to the manufacturer's instructions. The reverse transcription reaction was performed on 1 μg total RNA with SuperScript III Reverse Transcriptase (Invitrogen, Carlsbad, USA according to the manufacturer's instructions. The gene-specific primers used were described previously, or were designed using Primer3 software (http://frodo.wi.mit.edu/primer3/), (supplemental Table 2, supporting information). Gene expressions were performed on an iQ-Cycler (Bio-Rad, Hercules, CA) in triplicate with iQ-SYBR Green Supermix. The PCR program consisted of 10 min of incubation at 95 °C followed by 40 cycles of 15 s at 95 °C and 1 min at 60 °C where the fluorescence signal was measured. The specificity of the PCR amplification procedure was checked with a heat dissociation protocol (from 65 °C to 100 °C) after the final cycle of the PCR. The proportion of transcript present in the samples was calculated using the $2^{-\Delta\Delta Ct}$ method using GAPDH house-keeping for levels normalization [24]. The final results represent the relative amount of amplicon in SLE patient (fold increase) with the mean level of healthy controls transcripts.

2.12. *Statistical analysis*

Values are given as the mean ± standard error (SE), unless otherwise indicated. Comparisons of the means between two groups were performed with the Student's *t* test for normally distributed variables and the Mann–Whitney *U* test for non-normal variables. The Wilcoxon rank test was used for comparisons between patients and controls (Figs. 8 and 9). Fisher's exact test was used to compare two proportions. The one-way ANOVA test was used to compare mean values of three or more groups. In some cases the Kruskal–Wallis nonparametric test was used to compare medians instead. If the mean values were statistically significant by the ANOVA test, then the Tukey–Kramer test was used to compare all pairs of groups. Differences were considered statistically significant for P values <0.05. Analysis of the data was done using the GraphPad Prism version 5.04 software (GraphPad Software, Inc., San Diego, CA).

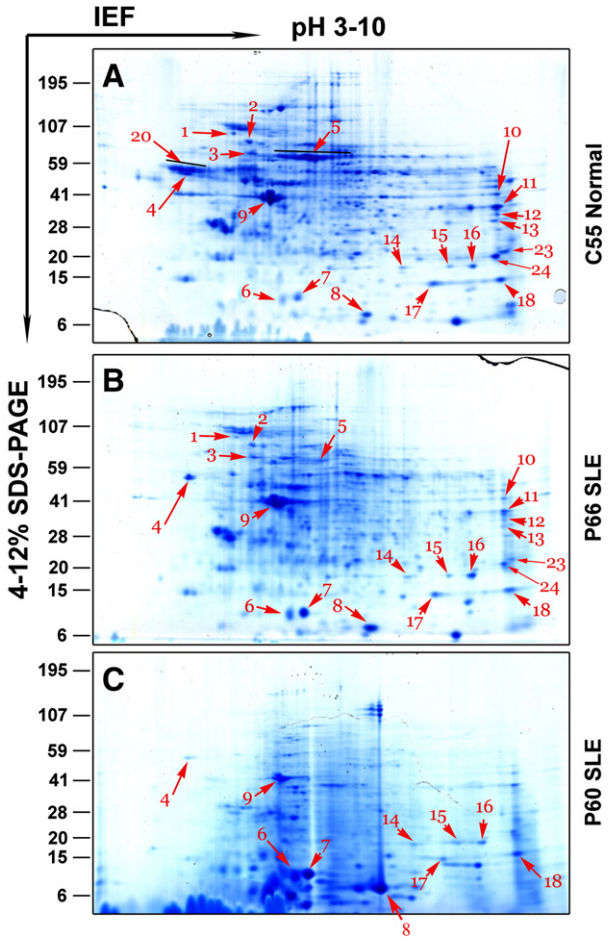

Fig. 1 – 2-DE analysis of peripheral blood mononuclear cells (PBMC) proteins from a healthy normal control C55 (A), and from two different SLE patients, P66 (B), and P60 (C). Post-nuclear PBMC proteins were separated by 2-DE as described in Materials and methods. 275 μg of protein was loaded per gel. Bio-Safe Coomassie staining. Some of the proteins that were consistently identified are marked on the gels (see also Table 1, and Suppl. Table 3). The lower regions of the 2-DE gels show the mixed SDS-ASB-14 micellar front, which is more prominent at the acidic extreme of the IPG. IPGs were pH 3–10. Note in panel A that spots in area 5 were identified by PMF as bovine serum albumin (Mascot score of 158, $P<0.05$), and spots in area 20, just above spot 4, were identified as alpha-2HS-glycoprotein also of bovine origin (Mascot score of 109, $P<0.05$). These contaminant proteins may have come from the 10% Fetal Bovine Serum (FBS) added to the medium during the PBMC isolation procedure. These spots were not detectable in panels B and C, in which PBMCs were washed in FBS-free RPMI instead.

3. Results and discussion

3.1. *Protein composition of PBMCs*

Plasma membrane and cytosolic proteins were extracted from PBMC lysates upon separation from intact nuclei and NP-40 insoluble material, and 2-DE gels were run for each sample as described in Materials and methods. A representative gel of a control and two SLE patients is shown in Fig. 1. In a first approach our goal was to identify as many different proteins as possible from either normal controls or SLE PBMCs to check for the protein composition of this heterogeneous cell population. To perform this, samples from 8 different controls, and 6 SLE patients were analyzed. A total of 354 out of 438 spots were successfully identified by PMF, with annotations of 166 spots representing 98 unique proteins identified by MS (Supplemental Table 3, and Supplemental Figs. 1–5, supporting information). The Human Protein Reference Database (http://www.hprd.org) was used to group the identified proteins according to their biological functions. Most proteins were classified in three categories: signal transduction/cell communication (36.9%), cell growth and/or maintenance (29.1%), and protein metabolism (19.4%) (Fig. 2A). The cellular component classification showed that most proteins were primarily located at the cytoplasm (64.1%), and to a lesser extent at the plasma membrane (10.7%), and other categories (Fig. 2B).

Knowledge of the mass and pI of the intact proteins obtained by 2-DE allows to discriminate between different isoforms and PTMs [25]. In this study, at least 29 proteins were resolved in more than 1 spot with similar Mr and different pI within each protein, suggesting the existence of PTMs (see MS data referred to PPIase A and Profilin-1 spots, Supplemental Figs. 6–8, supporting information). To note is that in SLE PBMCs the proportion of spot 14 relative to the total amount of PPIase A was significantly higher than that in Normal PBMCs (32.04% ± 3.8 versus 20.2% ± 3.6, $P = 0.0356$, t-test), which would suggest increased phosphorylation of PPIase A in these cells (Supplemental results, supporting information).

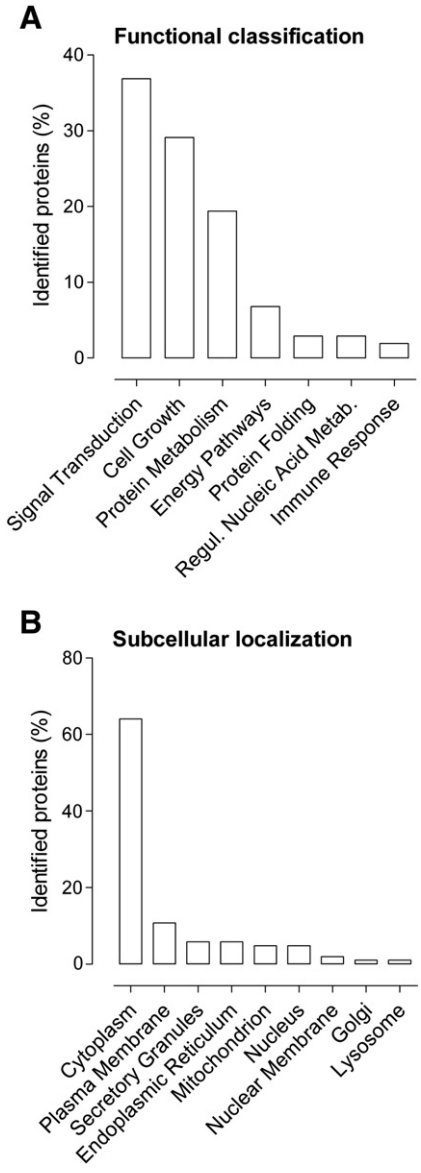

Fig. 2 – Protein ontology. Identified proteins were classified according to their (A) biological functions, and (B) expected subcellular localization.

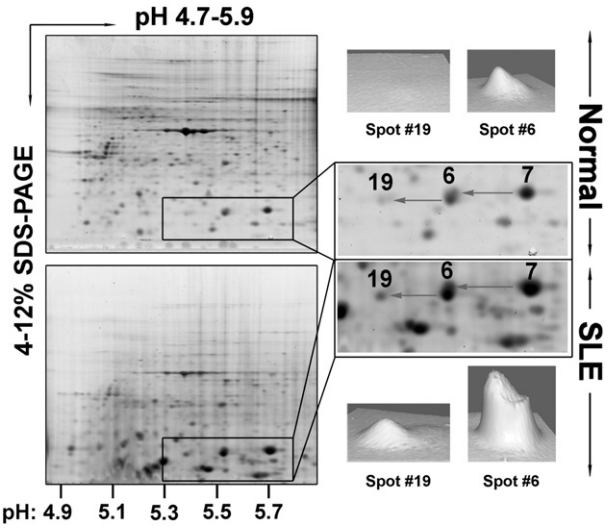

Fig. 3 – 2-DE analysis of peripheral blood mononuclear cells (PBMC) proteins from a healthy normal control (left upper panel), and from one SLE patient (left lower panel) using IPG strips of pH 4.7 to 5.9. Post-nuclear PBMC proteins were separated by 2-DE as described in Materials and methods. 275 μg of protein was loaded per gel. SYPRO-Ruby staining. Outlined regions in the lower region of the 2-DE gels are imaged enhanced to show the S100A9 spots (right middle panels). Arrows indicate the positions where the corresponding phosphorylated forms of S100A9-l (spot 7) and S100A9-s (lower part of spot 6) migrate. The right upper and lower panels are tridimensional representations of spots 19 and 6 to show their distinct shapes. The orientation of spot 6 in the tridimensional representation has been purposely changed from that in the 2-DE gel to better show the prominent protrusion, which is likely to be the phosphorylated form of S100A9-l.

3.2. *Identification of the two S100A9 isoforms and their phosphorylated forms*

Two proteins, actin and S100A9, also showed several spots that differed in both size and pI from their theoretical values, which suggested the presence of distinct isoforms and/or truncations (Supplemental Table 3, and Supplemental Fig. 1–5, supporting information). S100A9 exists in two isoforms of differing polypeptide chain lengths [26]. The low molecular weight form is termed S100A9 short (S100A9-s), and the high

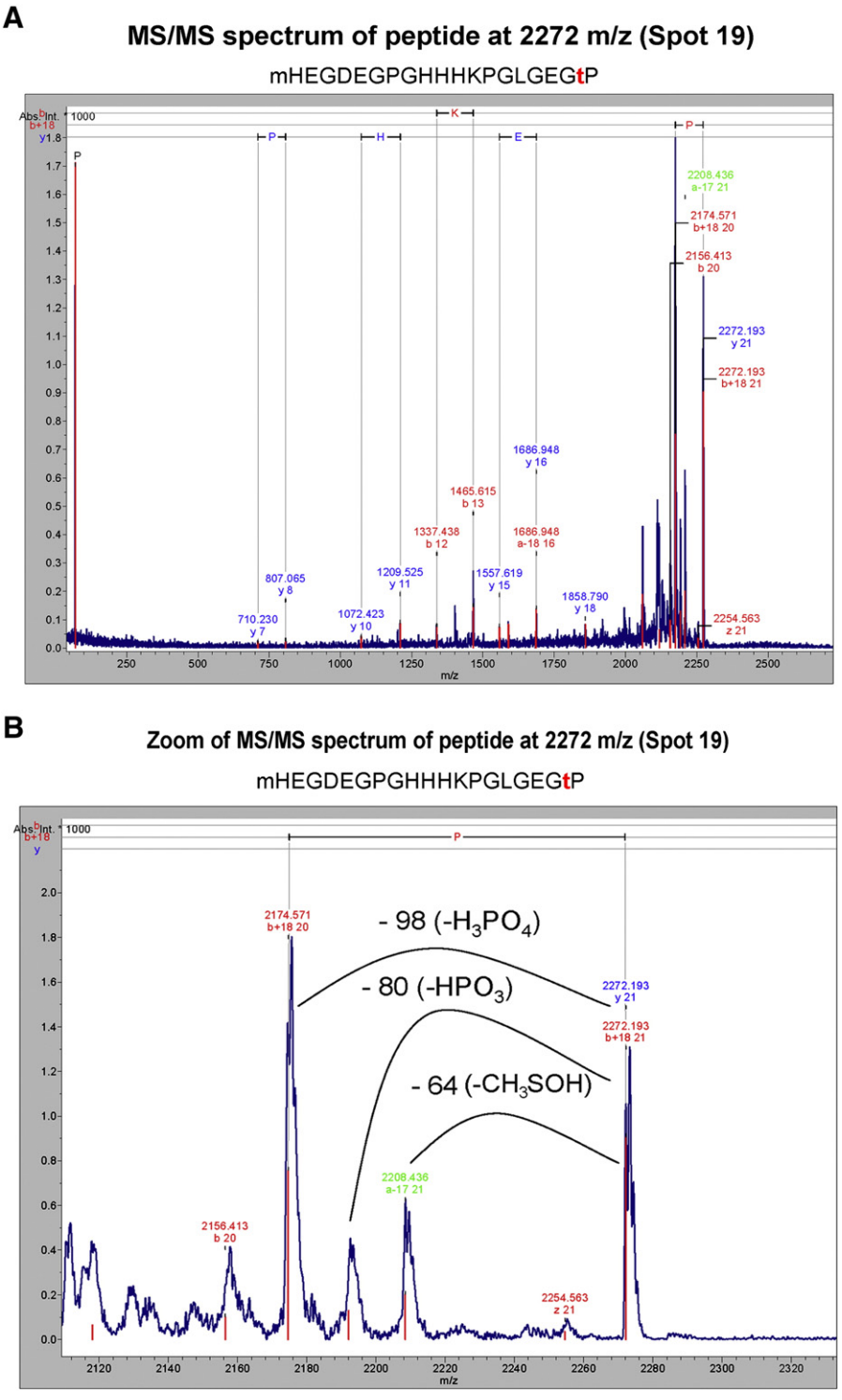

Fig. 4 – (A) MS/MS spectrum of peptide with ion signal at *m/z* 2272 from spot #19. The determined amino acid sequence is depicted on top, corresponding to the phosphorylated C-terminal peptide from S100A9. (B) Zoom of MS/MS spectrum of peptide at *m/z* 2272 from spot #19, showing a peak at *m/z* 2174, which corresponds with the neutral loss of 98 *m/z* (the mass of phosphoric acid, H_3PO_4) from the parent phosphorylated ion, and a peak at *m/z* 2192, which corresponds with the loss of 80 *m/z* (the mass of the phosphoryl group, $–HPO_3$).

molecular weight form S100A9 long (S100A9-l) [27,28]. S100A9-s lacks the first four amino acids (MTCK, single letter amino acid code); its polypeptide chain starts at the second methionine compared with that of the larger isoform S100A9-l, and they differ in only 463 Da. The two isoforms may also lose their respective N-terminal methionine residues and become acetylated [28]. Therefore, the lack of the first four or five amino acids results in the loss of Lys^4, which lowers 0.16 units the pI of S100A9-s relative to that of S100A9-l, as estimated using the ExPASy Compute pI/Mw tool, or 0.19 units as calculated by Edgeworth et al., [26]. Likewise, phosphorylation of S100A9-l at Thr^{113} lowers its pI 0.16 units [29]. As a result phosphorylated S100A9-l migrates just above the non-phosphorylated S100A9-s on 2-DE gels using IPG strips in the pH range of 3–10 as in Fig. 1. Overall these data suggested that spot 7 may correspond to S100A9-l, and spot 6 to a mixture of non-phosphorylated S100A9-s and phosphorylated S100A9-l (Fig. 1).

In an attempt to detect better the two S100A9 isoforms, proteins from Normal and SLE PBMC lysates were separated by 2-DE using IPG strips in the pH range of 4.7 to 5.9. As shown in Fig. 3, an additional spot was detected (spot 19), which exhibited the same apparent molecular mass but a lower pI than S100A9-s (spot 6). Moreover, in both Normal and SLE samples the three dimensional representation of spot 6 showed an asymmetrical shape with two overlapping peaks, which suggested the presence of two proteins. The upper peak had an electrophoretic mobility similar to that of spot 7 and a slightly more basic pI than the lower and more prominent peak. The upper part of spot 6 may correspond to the phosphorylated form of S100A9-l, and the lower one to nonphosphorylated S100A9-s. In contrast, the symmetrical 3-D shape of spot 19 suggested the presence of a single protein, which may correspond to the phosphorylated form of S100A9-s (see also Fig. 6A).

S100A9 was reported previously to be phosphorylated exclusively on Thr^{113} [22,30]. MALDI-TOF MS analysis of the tryptic digests from spots 6, 7, and 19 confirmed the presence of S100A9 in all digests (Mascot scores: 94, 84 and 68, respectively, $P<0.05$). In all spectra, a signal that could be assigned to the C-terminal 21-aa, tryptic peptide containing Thr^{113} and an oxidized methionine was observed at *m/z* 2192.01, 2191.95, and 2191.94 (calculated *m/z* 2191.958) for spots 6, 7, and 19, respectively (Supplemental Fig. 4, supporting information). Additional ions at 2272.00 *m/z*, and at 2271.93 *m/z* were observed in the spectra from spots 6, and 19, respectively, but not from spot 7 (Supplemental Fig. 9, supporting information). These results suggest that the C-terminal 21-aa tryptic peptide of S100A9 from spots 6, and 19 was additionally modified by phosphorylation.

To confirm this point, tryptic digests of spot 19 were subjected to MALDI-LIFT/TOF analysis. The fragmentation spectra of the signal observed at *m/z* 2272 matched the expected ^{94}mHEGDEGPGHHHKPGLGEGtP^{114} sequence (Fig. 4A) (Mascot score=48.2; Supplemental Fig. 10, supporting information) and showed intense, characteristic ions derived from neutral losses of phosphoric (98 uma) and metaphosphoric (80 uma) acids (Fig. 4B). On the other hand, fragmentation of ion at 2192 *m/z* from spot 7 yielded a fragmentation pattern that matched the sequence ^{94}mHEGDEGPGHHHKPGLGEGTP^{114} (Fig. 5), corresponding to the non-phosphorylated C-terminal peptide from S100A9 (Mascot score: 55.7; Supplemental Fig. 11, supporting information).

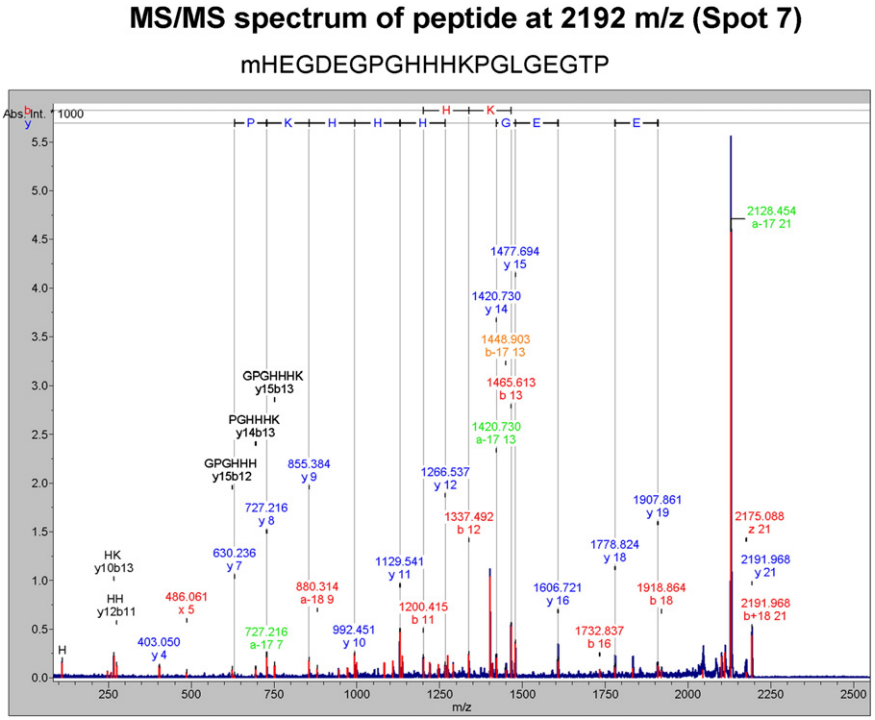

Fig. 5 – MS/MS spectrum of peptide with ion signal at *m/z* 2192 from spot #7. The determined amino acid sequence is depicted on top, corresponding to the unphosphorylated C-terminal peptide from S100A9.

3.3. *Increased phosphorylation of S100A9 in SLE PBMCs upon stimulation with PMA and Ionomycin*

Edgeworth and coworkers [22] have shown that activation of neutrophils and monocytes with calcium ionophore induces phosphorylation of S100A9 on Thr^{113}. To assess whether the calcium ionophore, ionomycin, induces increased phosphorylation of S100A9 in SLE PBMCs, cells were incubated with or without ionomycin for 10 min at 37 °C and cell lysates were analyzed by 2-DE. After electrophoresis, gels were stained with Pro-Q Diamond, which is a dye specific for phosphorylated proteins [31], followed by SYPRO Ruby for total-protein staining. Fig. 6A shows that in unstimulated cells only spots 19 and 6 were stained with Pro-Q Diamond, whereas the three S100A9 spots were stained with SYPRO Ruby, indicating that only the more acidic forms of S100A9 were phosphorylated. In unstimulated cells the ratio of the fluorescence intensity of the Pro-Q Diamond signal (D) relative to the SYPRO Ruby signal (S) was of 4.3 for spot 19, and 1.6 for spot 6, respectively, which was consistent with the data of Fig. 3 that indicated that spot 6 was a mixture of phosphorylated S100A9-l and nonphosphorylated S100A9-s, whereas spot 19 was exclusively the phosphorylated

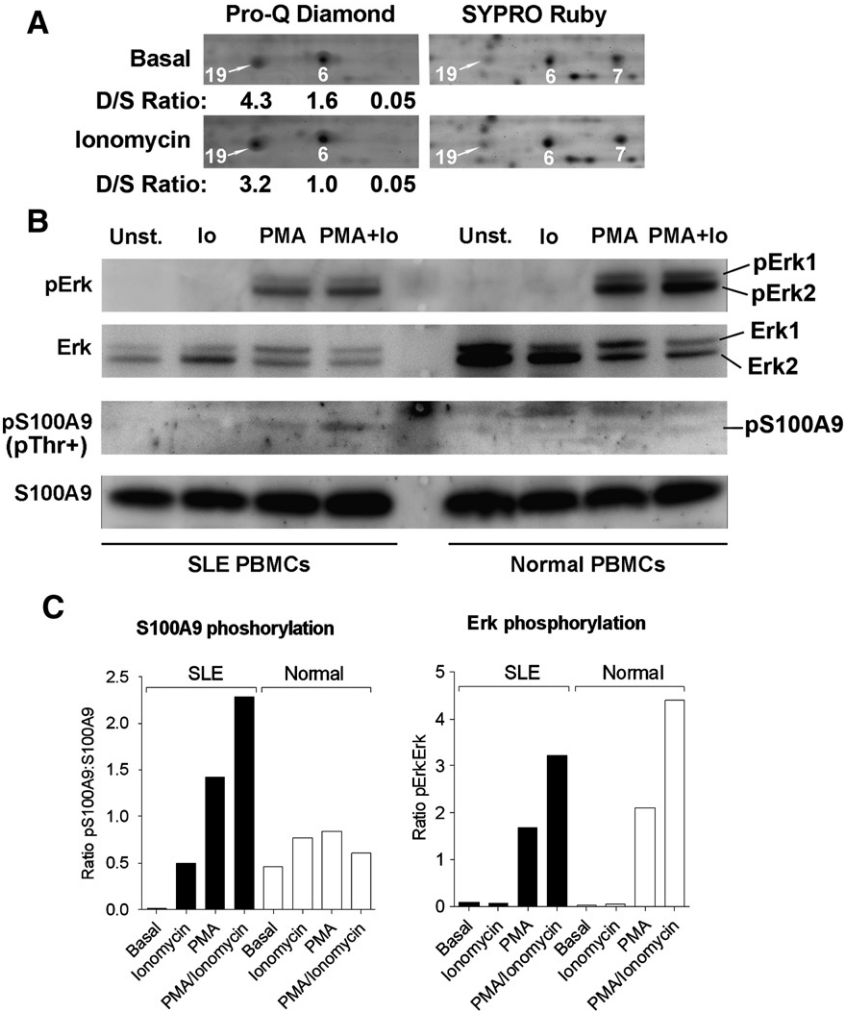

Fig. 6 – Increased phosphorylation of S100A9 in SLE PBMCs. (A), PBMC were incubated with or without Ionomycin for 10 min at 37 °C as indicated in Materials and methods, and cell lysates were analyzed by 2-DE. After electrophoresis, gels were stained with Pro-Q Diamond (left panels), followed by SYPRO Ruby for total-protein staining (right panels). Only the region of interest is shown. For each S100A9 spot, the D/S ratio of the fluorescence intensity of the Pro-Q Diamond signal (D) to that of the SYPRO Ruby signal (S) is indicated below the Pro-Q Diamond-stained gels (left panels). This is a representative experiment out of two performed in PBMC from two different SLE patients. (B), PBMCs from a SLE patient (lanes 1–4), and a Normal control (lanes 5–8) were left unstimulated (lanes 1 and 4), or stimulated with Ionomycin alone (lanes 2 and 6), with PMA (lanes 3 and 7), or with PMA + Ionomycin (lanes 4 and 8) for 10 min at 37 °C. PBMC were then lysed and proteins were separated by SDS-PAGE and transferred to PVDF membranes. The lower part of the membranes were immunoblotted with an anti-phosphothreonine specific mAb (third panel), followed by an anti-S100A9 specific polyclonal antibody (fourth panel). The upper part of the membrane was immunoblotted with an anti-phospho Erk (Thr^{185}/Tyr^{187}) specific antibody (first panel), followed by an anti-Erk (total protein) polyclonal antibody (second panel). (C), in left panel the ratio of phosphoS100A9 relative to total S100A9 is shown. In right panel the phosphoErk/total Erk ratio is shown. Solid bars, SLE PBMC; open bars, Normal control PBMC. This is a representative experiment out of two.

form of S100A9-s. Upon ionomycin treatment the D/S ratio was of 3.2 for spot 19, and 1.02 for spot 6, which indicated a decrease in the phosphorylation of those proteins of 27% and 38%, respectively.

p38 MAPK is the kinase that phosphorylates S100A9 in monocytes [32], and in neutrophils [30], in a process that requires elevation of intracellular calcium levels [32]. In T cells activation of p38 MAPK (phosphorylation) is readily induced by stimulation with PMA/ionomycin [33]. To assess whether S100A9 results phosphorylated in SLE PBMCs under conditions of optimal p38 MAPK activation, cells were stimulated with medium, ionomycin (200 ng/ml), PMA (400 ng/ml), or PMA (400 ng/ml) + ionomycin (200 ng/ml), and then incubated for 10 min at 37 °C as described [22]. Since S100A9 was the only phosphorylated protein at 14 kDa detected after Pro-Q Diamond staining, proteins were separated by 1-D SDS-PAGE, transferred to a PVDF membrane and Western-blotted with an anti-phosphothreonine specific antibody. As shown in Fig. 6B (third panel), ionomycin alone was relatively inefficient in inducing Thr-phosphorylation of S100A9 in both the SLE and Normal PBMC. In contrast, PMA alone induced a stronger increase in Thr-phosphorylation of S100A9 in SLE than in Normal PBMC, which was further increased upon the simultaneous stimulation with PMA and ionomycin

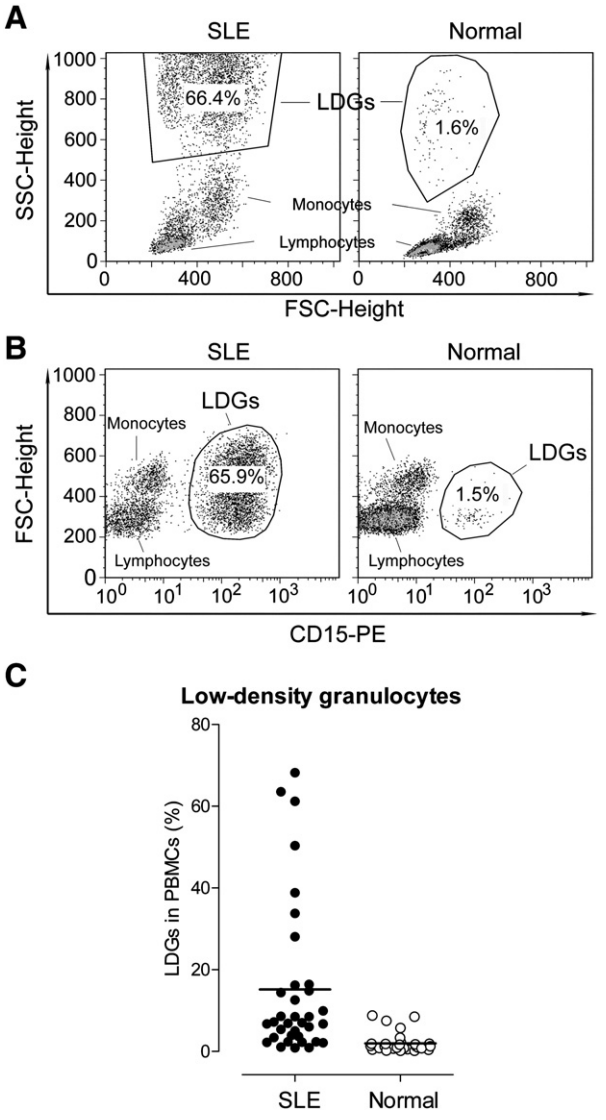

Fig. 7 – Increased presence of low-density granulocytes in SLE PBMC. (A) Dot plots of the Forward (X-axis), and Scatter (Y-axis) characteristics of PBMC from a SLE patient (left panel), and from a Normal control (right panel). (B), Dot plots of CD15 staining (X-axis) versus Forward characteristics (Y-axis) of PBMC from the same SLE patient (left panel), and Normal control (right panel) as in (A). (C), Dot diagram of the percentage of low-density granulocytes in SLE (closed circles), and Normal controls (open circles). Each symbol represents one patient or control, and the bar within each group represents the mean percentage value.

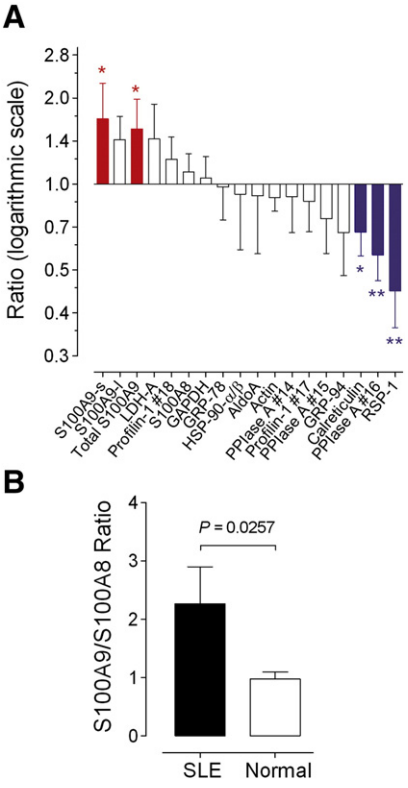

Fig. 8 – Relative protein levels in SLE PBMC extracts separated by 2-DE gels as compared with those in Normal PBMC. (A) The intensity value for each individual spot in 2-DE gels from 14 SLE patients was normalized to the mean of the intensity values obtained in 15 Normal controls and expressed as a ratio or fold-change. The Y axis has been converted to a logarithmic scale to better appreciate the increased or decreased protein expression setting a baseline of Y = 1.0. Bars represent the Mean + SEM for each protein spot. P values that are statistically significant (Wilcoxon Signed Rank Test) are shown as follows: * is for a P value from 0.01 to 0.05, and it is considered significant. ** is for a P value from 0.001 to 0.01, and it is considered very significant. (B) The S100A9/S100A8 ratio was calculated in each individual 2-DE gel of PBMC extracts used in (A). Fold-changes are given as the ratio of the relative volumes of S100A9 spots (S100A9-s + S100A9-l) over the S100A8 spot. The data represent the Mean + SEM in SLE (closed bar), or Normal (open bar). The P value is for the comparison of the median S100A9/S100A8 ratio of SLE versus Normal (Mann–Whitney test).

(Fig. 6C, left panel). The phosphorylated band was indeed S100A9 because it was identified by reblotting the same membrane with an anti-S100A9 specific antibody, which reacted with a protein at the same apparent molecular weight (Fig. 6B, lower panel). This was confirmed by running in parallel an aliquot of the same sample and upon staining with SYPRO Ruby, the band at 14 kDa was excised, trypsin-digested and analyzed by MALDI-TOF MS. Two ions at 2192 *m/z* and at 2272 *m/z*, corresponding to the unphosphorylated and phosphorylated C-terminal S100A9 peptides, were detected in samples from PMA stimulated SLE PBMCs but not from Normal PBMCs (data not shown). Therefore, these data demonstrate that in SLE PBMCs S100A9 phosphorylation is more efficiently induced when both PMA and ionomycin are present at the same time than separately. To note is that either PMA alone or in combination with ionomycin induced a stronger phosphorylation of Erk1/2 in Normal than in SLE PBMCs (Fig. 6B, upper panel, and Fig. 6C, right panel), which is in agreement with the observed decreased MAP kinase activity observed in SLE T cells [2].

3.4. *Presence of low-density granulocytes (LDGs) in SLE PBMCs*

LDGs, which are proinflammatory and display pathogenic features, including the capacity to synthesize type I IFNs have been recently characterized in SLE patients [34]. In another study, it has been shown that children with active SLE can be distinguished by a remarkably homogeneous gene expression pattern with overexpression of granulopoiesis-related genes, which are likely related with the presence of low-density mature granulocytes and/or immature granulocytes in their PBMCs [35]. In our study, SLE PBMCs from adults also showed a population of highly granular cells, which was clearly distinguishable from monocytes and lymphocytes by flow cytometry analysis based in their distinct forward (FSC) and side scatter (SSC) characteristics (Fig. 7A, left panel). These cells were also present in PBMCs from normal controls, although to a very low proportion (Fig. 7A, right panel). The monocyte/lymphocyte pools and the low-density granulocytes could be clearly distinguished in SLE samples based upon expression of CD15, which is a specific marker for neutrophils and eosinophils (Fig. 7B). Indeed, there was an almost perfect correlation between the percentage of $CD15^{+}$ cells and the percentage of SSC/FSC^{high} in SLE PBMCs ($r=0.9993$, $P<0.0001$, $n=27$, Pearson's test). The forward and side scatter profile was used to determine the relative levels of low-density granulocytes in PBMCs from SLE patients and healthy individuals (Fig. 7C). Low-density granulocytes in SLE preparations represented an average of 15% of total PBMCs, with a range of 0.9–68% ($n=35$). By comparison, PBMCs from 31 healthy controls showed an average of 2% low-density granulocytes (0.2–8.8% range, $P<0.0001$, Mann–Whitney test). These data were confirmed by CD15 expression (data not shown).

3.5. *Identification of a pattern of differentially expressed proteins in SLE PBMCs*

To test whether S100A9 protein expression was up-regulated in SLE PBMCs, a total of 29 gel images from 15 Controls and 14 Patients were analyzed using the PDQuest software. The intensity value for each individual spot in 14 SLE patients was normalized to the mean of the intensity values obtained in 15 normal controls. Only the calcium-binding proteins S100A9-s and S100A9-l, and the alpha chain of L-lactate dehydrogenase A chain (LDH-A, spot 12, Fig. 1) showed mean fold-changes closer to or above 1.5 relative to normal controls (Fig. 8A), with 5 and 4 out of 14 SLE patients showing S100A9 or LDH-A protein levels above the cut-off value of 1.5, respectively. The data indicated that the differences in expression of total S100A9 (S100A9-s+S100A9-l), or S100A9-s were statistically significant (Wilcoxon test). In contrast, there were a number of proteins as calreticulin (spot 4), PPIase A (spot 16) and Ras suppressor protein 1 (RSP-1, spot 13), with mean fold-changes closer to 0.5 that were statistically significant (Fig. 8A), indicating down-regulated expression.

Table 1 – Crossed correlation coefficients computed among the 17 proteins of Fig. 1 in SLE patients.

	Spot no.[a]	8	6	7	1	2	3	9	4	10	11	13	12	17	18	14	15
S100A8	**8**																
S100A9-s	**6**	0.81[a]															
S100A9-l	**7**	0.77[b]	0.86														
GRP-94	**1**	−0.45	**−0.76**[c]	**−0.66**													
HSP90α/β	**2**	−0.20	−0.48	−0.41	0.75												
GRP-78	**3**	−0.50	**−0.58**	−0.40	0.69	0.71											
Actin	**9**	−0.50	**−0.69**	**−0.63**	0.72	0.65	0.61										
Calreticulin	**4**	0.14	−0.23	0.00	0.50	0.65	0.55	0.38									
Aldo A	**10**	−0.33	−0.39	**−0.54**	0.60	0.53	0.63	0.32	0.36								
GAPDH	**11**	−0.48	−0.49	**−0.66**	0.65	0.59	0.66	0.45	0.18	0.91							
RSP-1	**13**	**−0.56**	**−0.56**	**−0.79**	0.25	0.14	0.11	0.36	−0.32	0.29	0.36						
LDHA	**12**	−0.35	−0.31	−0.50	0.39	0.30	0.48	0.08	0.10	0.72	0.79	0.31					
Prof. 1 #17	**17**	0.17	−0.15	−0.05	0.34	0.56	0.31	0.50	0.78	0.36	0.10	−0.25	−0.05				
Prof. 1 #18	**18**	−0.13	−0.01	0.02	0.11	0.13	0.43	−0.24	0.12	0.19	0.52	−0.14	0.57	−0.02			
PPIA #14	**14**	0.45	0.24	0.15	−0.06	0.23	0.00	0.04	0.50	0.09	0.08	−0.29	0.26	0.62	0.12		
PPIA #15	**15**	0.58	0.37	0.39	−0.22	−0.06	−0.27	−0.09	0.44	−0.25	−0.33	**−0.64**	−0.14	0.65	−0.11	0.84	
PPIA #16	**16**	0.41	0.05	0.16	0.23	0.47	0.25	0.17	0.69	0.27	0.12	−0.34	−0.16	0.52	0.05	0.44	0.39

[a] Spot numbers (in bold) correspond to those depicted in Fig. 1.

[b] Positive correlation coefficients, r, which are statistically significant are highlighted in bold red. The *P* values ranged from $P=0.0497$ for $r=0.53$ up to $P<0.001$ for $r=0.91$. *P* values were obtained using Spearman's correlation test ($n=14$ SLE patients).

[c] Negative correlation coefficients are highlighted in bold blue. The *P* values ranged from $P=0.0449$ for $r=-0.54$ up to $P=0.0016$ for $r=-0.76$.

It is assumed that protein synthesis of S100A9 and S100A8 is coordinately regulated [36]. However, in Smad4-negative tumors, the recruited myeloid cells express S100A9, but exhibit lower S100A8 expression [37], as it occurs in acute inflammatory reactions [38]. In SLE PBMCs the S100A9:A8 ratio was significantly higher than that in Normal PBMCs (Fig. 8B), which may reflect the differentiation state of the myeloid cells expressing these proteins.

A deeper examination of the data suggested that increased expression of S100A9 or LDH-A did not occur in the same samples and it was indicative of distinct non-overlapping protein profiles. Table 1 shows several clusters of proteins with highly significant correlations between them. Thus, there was a positive correlation of S100A9-l protein levels with S100A8 (r=0.77), and indeed with S100A9-s (r=0.86), whereas there was a significant negative correlation of either S100A9-l or S100A9-s, or both with the three heat-shock proteins (GRP-94, HSP 90α/β (spot 2), and GRP-78 (spot 3), actin (spot 9), RSP-1, Fructose-bisphosphate aldolase A (AldoA, spot10), and Glyceraldehyde-3-phosphate dehydrogenase (GAPDH, spot 11). The three heat-shock proteins, actin, Aldo A (spot 10) and GAPDH showed a positive correlation between them. In contrast, calreticulin correlated positively with Hsp90α/β, GRP-78, Profilin-1, spot 17, and with PPIase A, spot 16, which suggested a distinct set of correlations. Likewise, RSP-1 did not show any positive correlation with any of the proteins tested, while LDH-A protein levels correlated positively with Profilin-1 (spot 18), AldoA, and GAPDH (spot 11). Although some of these proteins are considered housekeeping, it is interesting to note that GAPDH, and AldoA are differentially expressed in PHA-activated T cells as compared with resting T cells [39].

3.6. *Validation by Western blotting and RT-PCR analysis*

To check the validity of the results obtained by 2-DE and mass spectrometry, Western blotting experiments were conducted in a larger number of SLE (n=30) and Normal control (n=30) PBMC lysates (Fig. 9). HSP 90α/β, HSP 70, PPIase A, S100A9, S100A8, and Actin were chosen for analysis due to relevance considerations and availability of good antibodies. The data showed that S100A9 median values were significantly higher in SLE than in Normal control PBMC lysates. In contrast, HSP 90α/β, HSP 70, and PPIase A median values were significantly lower in SLE than in Normal control PBMC lysates (Fig. 9B). Note in Fig. 9A that SLE PBMC lysates showing the highest S100A9, and S100A8 protein levels as P60 and P61 also showed the lowest relative levels of HSP 90α/β. In fact, there was a positive correlation between S100A8 and S100A9 protein levels (r=0.6931, P<0.0001), and a negative correlation between HSP 90α/β and either S100A8 (r=−0.3726, P=0.0426), or S100A9 (r=−0.6080, P=0.0004), whereas HSP 90α/β and HSP 70 correlated positively between them (r=0.5567, P=0.0014). In contrast, a good correlation was found between the S100A9 protein levels

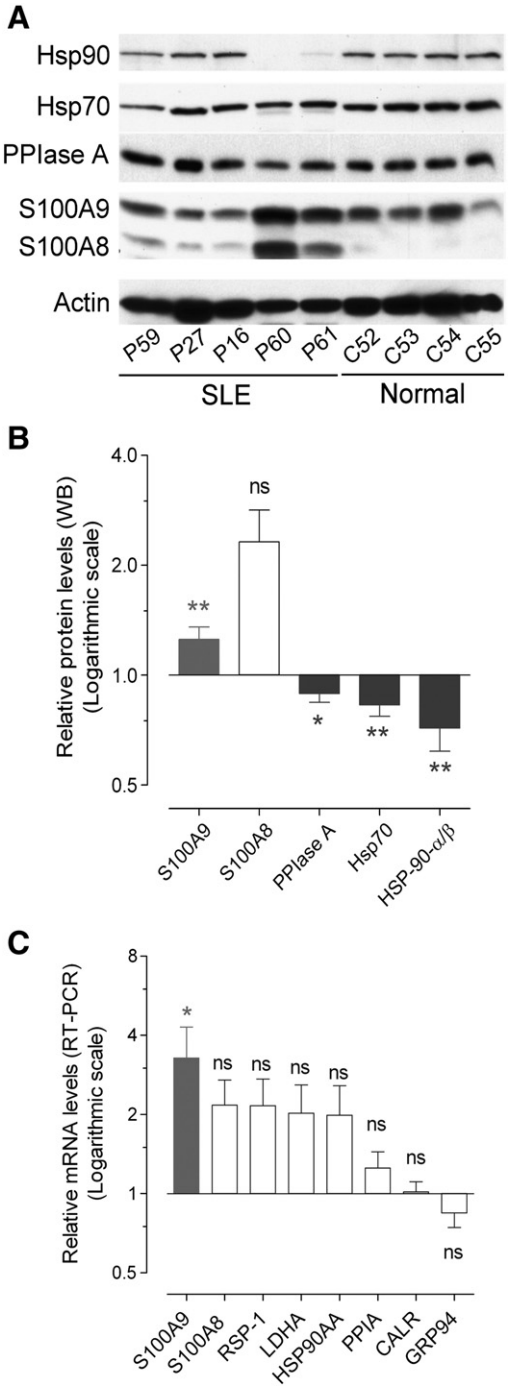

Fig. 9 – Western blot and RT-PCR analyses. (A), PBMC from SLE patients or Normal controls were lysed in 1% NP-40 lysis buffer as described in Materials and methods. The soluble fractions were diluted in 3× SDS sample buffer and proteins were separated by 15% SDS-PAGE, transferred to PVDF membranes and immunoblotted for the indicated proteins on the left of the panel. (B), Relative protein levels of the indicated proteins detected by Western blot in 30 SLE PBMC lysates relative to the mean value in 30 Normal control PBMC lysates (fold-increase). (C), Transcript levels detected by quantitative real-time PCR in each SLE PBMC relative to the mean of transcript levels in Normal controls (fold-increase). Bars in (B) and (C) represent Mean+SEM. P values (Wilcoxon Signed Rank Test) are shown as follows: * is for a P value from 0.01 to 0.05, and it is considered significant. ** is for a P value from 0.001 to 0.01, and it is considered very significant. ns: Not significant.

in SLE PBMCs and the percentage of $CD15^+$ PBMCs (r=0.7382, P=0.0011, n=16), which strongly suggested that the increased expression of S100A9 in SLE PBMCs was in fact a good indicator for the presence of circulating low-density granulocytes.

Quantitative real-time PCR analysis in a completely different set of 14 SLE patients showed that expression of S100A8 and S100A9 mRNA was increased in SLE PBMCs relative to Normal controls (2.1 and 3.3 mean fold-increase, respectively), with 5 and 6 out of 14 SLE PBMC samples showing S100A8, or S100A9 mRNA levels above the cut-off value of 1.5, respectively (Fig. 9C). Increased mRNA expression was also observed for RSP-1 (2.2), LDHA (2.02), HSP90A (1.98), and to a lesser extent for PPIA (1.25). In contrast, the same samples showed slight decreased mean mRNA levels for GRP94 (0.84) and no changes for CALR expression (1.02). The mean mRNA levels for GRP94 (0.84±0.1) resembled the relatively low mean protein levels for GRP-94 detected by 2-DE (0.68±0.2). In contrast, RSP-1 mean mRNA levels (2.2±0.6) did not correlate with the respective mean protein levels detected on 2-DE gels (0.65±0.1).

Although only SLE S100A9 median values were statistically significant relative to that of Normal controls, there was a strong positive relationship between S100A8 and S100A9 mRNA levels (r=0.8198, P=0.0003) but not with any of the other genes tested. In contrast, LDHA mRNA levels correlated very well with the other genes tested: RSP-1 (r=0.9373, P<0.0001), PPIA (r=0.8965, P<0.0001), HSP90A (r=0.8405, P=0.0002), GRP94 (r=0.6132, P=0.0197), and CALR (r=0.6117, P=0.0201).

3.7. *Increased concentration of calprotectin in SLE plasma. Correlation with S100A9 expression in SLE PBMCs*

S100A9 and its binding partner, S100A8, are highly expressed in neutrophils comprising up to 30% of the total cytosolic protein mass in these cells. Monocytes contain about 40-fold less of these proteins than do neutrophils [26]. Moreover, the S100A8/A9 heterodimer or calprotectin is released from phagocytes and amplifies the endotoxin-induced inflammatory response. Therefore, we tested whether plasma levels of calprotectin were increased in SLE patients, and whether there was any correlation with the increased S100A9 and S100A8 expression in SLE PBMCs. As expected plasma levels of S100A8/A9 were significantly raised in SLE patients as compared with normal controls (Fig. 10A). However, S100A8/A9 plasma levels in SLE correlated with intracellular levels of S100A9 (Fig. 10B), but not with those of S100A8 (Fig. 10C).

The data of this study suggest a putative model of action, in which there is a link between increased plasma levels of S100A8/S100A9, increased S100A9 expression in SLE PBMCs, and the increased proportion of low-density granulocytes in these cells. Mature neutrophils recruited from blood to the inflammatory sites by immobilized immune complexes could lead to release of S100A9 locally, which can contribute via activation of p38 and JNK to the degranulation of neutrophils [40]. These cells are less dense that resting neutrophils and can produce higher amounts of IFN-α [34], which may in turn cause the arrest of granulocyte maturation [41], and, therefore, may further promote the increased presence of circulating low-density granulocytes. Phosphorylation of S100A9 may occur at this point induced by IFN-α, or by fMLP. Increased phosphorylation of PPIase A (supplemental Fig. 6) may be the consequence of TLR ligation by S100A9, which may induce increased expression of CXCR4 and further activation of the CXCL12/CXCR4 axis [42]. It is noteworthy that the relative concentration of PPIase A in SLE PBMCs correlates with the plasma levels of IL-6 and IL-13 in these patients (Supplemental Table 4, supporting information). In this sense, secreted PPIase A is the main ROS-induced

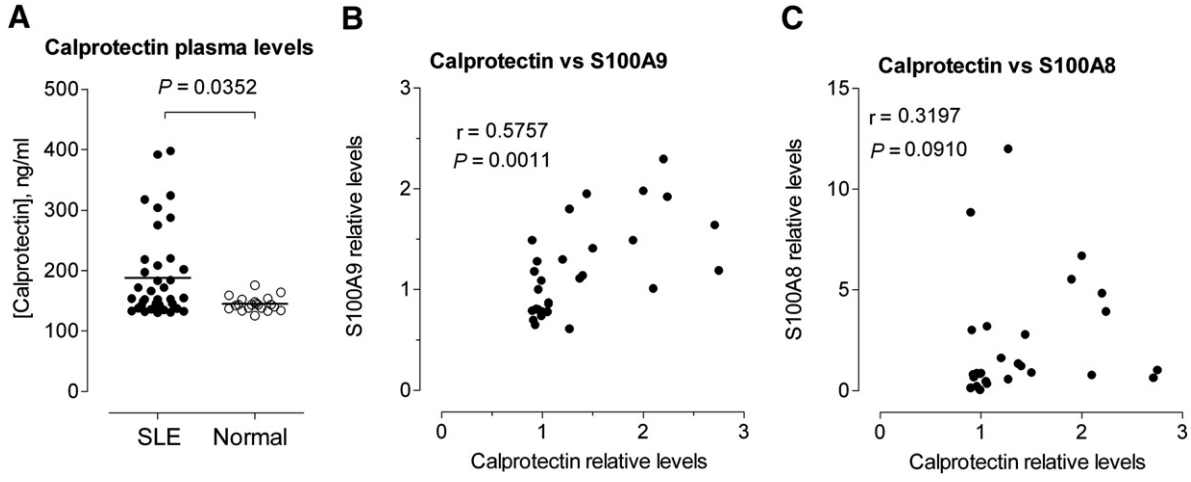

Fig. 10 – Increased calprotectin plasma levels in SLE patients. (A) Dot diagrams of calprotectin plasma levels quantified by ELISA in SLE patients (closed circles), and Normal controls (open circles). Each symbol represents one patient or control, and the bar within each group represents the mean value. *P* value is for the comparison of the median calprotectin plasma levels in SLE versus Normal (Mann–Whitney test). (B) Dot plot of calprotectin plasma levels (X-axis) versus S100A9 protein levels (Y-axis) in PBMC from SLE patients. (C) Dot plot of calprotectin plasma levels (X-axis) versus S100A8 protein levels (Y-axis) in PBMC from SLE patients. Calprotectin plasma level of each SLE patient was normalized relative to the mean value of the Normal control (fold-increase). Each symbol represents one SLE patient. Spearman's rank correlation coefficients (r) and significance levels (P) are in indicated in (B) and (C).

factor that enhances the inflammatory activity of monocytes/macrophages in atherosclerotic plaque, acts as a potent monocyte chemoattractant and induces increased IL-6 production by monocytes [43,44].

4. Conclusions

Significant and specific differences in protein expression have been found in SLE PBMCs as compared with those of Normal control PBMCs. Some of these differences are due to changes in the abundance of specific leukocyte subpopulations and not necessarily due to a defective regulation of protein or gene expression. The 2-DE and MS approach used in this study allowed us to detect the two unmodified S100A9 protein forms, S100A9-l and S100A9-s, which stem from alternate start Met codons, and the phosphorylation levels for each S100A9 form. Further, the MS/MS data precisely localize the phosphorylation to the penultimate residue (Thr^{113}) of the protein. Last, this approach underscores a proteomic signature for the abnormal presence of activated low-density granulocytes in SLE PBMCs.

Disclosure

None of the authors has any potential financial conflict of interest related to this manuscript.

Acknowledgements

This work was supported in part by the European Commission in collaboration with the following Funding Agencies: Ministerio de Ciencia e Innovación (MICINN) del Gobierno de España (SAF2005-06056-C02-01, and SAF2008-03685) (to J.S.), Consejería de Economía, Innovación y Ciencia de la Junta de Andalucía (P05-CVI-00908, and P08-CTS-04046) (to J.S.), and Ministerio de Sanidad, Política Social e Igualdad (MSPSI) ISCIII-FIS, Grants: FIS03/0389; UIPY-1465/07; MICINN-ISCIII-FIS-Grant: FIS06/1502, (to M.Z.), and MICINN-CSIC; Grant number: PI-200820I216 (to M.Z.). E.J.P. and R.P. were supported by grant-contracts from MICINN. S.G.R. was supported by a JAE-Doc contract. E.Z. and A.R.-V. were suported by felllowship-contracts from the Consejería de Economía, Innovación y Ciencia de la Junta de Andalucía.

We thank Pilar Navarro-Cuesta, and Salvador J. Guerrero-Fernández from the IPBLN, and Blanca Martínez-López from the Hospital Clínico for their technical assistance. The proteomic protein identification by LC-MS/MS analysis was carried out in the LP-CSIC/UAB, a member of ProteoRed network.

Appendix A. Supplementary data

Supplemental figures and tables are available free of charge via the Internet at ScienceDirect: http://www.sciencedirect.com. Supplementary data to this article can be found online at doi:10.1016/j.jprot.2011.12.020.

REFERENCES

[1] Janeway CA, Travers P, Walport M, Shlomechik M. Immunobiology. 5th ed. New York: Garland Publishing; 2001.
[2] Kammer GM, Perl A, Richardson BC, Tsokos GC. Abnormal T cell signal transduction in systemic lupus erythematosus. Arthritis Rheum 2002;46:1139–54.
[3] Kong PL, Odegard JM, Bouzahzah F, Choi JY, Eardley LD, Zielinski CE, et al. Intrinsic T cell defects in systemic autoimmunity. Ann N Y Acad Sci 2003;987:60–7.
[4] Rozzo SJ, Allard JD, Choubey D, Vyse TJ, Izui S, Peltz G, et al. Evidence for an interferon-inducible gene, Ifi202, in the susceptibility to systemic lupus. Immunity 2001;15:435–43.
[5] Wakeland EK, Liu K, Graham RR, Behrens TW. Delineating the genetic basis of systemic lupus erythematosus. Immunity 2001;15:397–408.
[6] Kuruto R, Nozawa R, Takeishi K, Arai K, Yokota T, Takasaki Y. Myeloid calcium binding proteins: expression in the differentiated HL-60 cells and detection in sera of patients with connective tissue diseases. J Biochem 1990;108:650–3.
[7] Haga HJ, Brun JG, Berntzen HB, Cervera R, Khamashta M, Hughes GR. Calprotectin in patients with systemic lupus erythematosus: relation to clinical and laboratory parameters of disease activity. Lupus 1993;2:47–50.
[8] Soyfoo MS, Roth J, Vogl T, Pochet R, Decaux G. Phagocyte-specific S100A8/A9 protein levels during disease exacerbations and infections in systemic lupus erythematosus. J Rheumatol 2009;36:2190–4.
[9] Lood C, Stenstrom M, Tyden H, Gullstrand B, Kallberg E, Leanderson T, et al. Protein synthesis of the pro-inflammatory S100A8/A9 complex in plasmacytoid dendritic cells and cell surface S100A8/A9 on leukocyte subpopulations in systemic lupus erythematosus. Arthritis Res Ther 2011;13:R60.
[10] Urban CF, Ermert D, Schmid M, Abu-Abed U, Goosmann C, Nacken W, et al. Neutrophil extracellular traps contain calprotectin, a cytosolic protein complex involved in host defense against *Candida albicans*. PLoS Pathog 2009;5:e1000639.
[11] Frosch M, Vogl T, Waldherr R, Sorg C, Sunderkotter C, Roth J. Expression of MRP8 and MRP14 by macrophages is a marker for severe forms of glomerulonephritis. J Leukoc Biol 2004;75:198–206.
[12] Dai Y, Hu C, Huang Y, Huang H, Liu J, Lv T. A proteomic study of peripheral blood mononuclear cells in systemic lupus erythematosus. Lupus 2008;17:799–804.
[13] Loser K, Vogl T, Voskort M, Lueken A, Kupas V, Nacken W, et al. The Toll-like receptor 4 ligands Mrp8 and Mrp14 are crucial in the development of autoreactive CD8+ T cells. Nat Med 2010;16:713–7.
[14] Wang L, Dai Y, Qi S, Sun B, Wen J, Zhang L, et al. Comparative proteome analysis of peripheral blood mononuclear cells in systemic lupus erythematosus with iTRAQ quantitative proteomics. Rheumatol Int 2010, doi:10.1007/s00296-01-1625-9.
[15] Haudek VJ, Slany A, Gundacker NC, Wimmer H, Drach J, Gerner C. Proteome maps of the main human peripheral blood constituents. J Proteome Res 2009;8:3834–43.
[16] Tan EM, Cohen AS, Fries JF, Masi AT, McShane DJ, Rothfield NF, et al. The 1982 revised criteria for the classification of systemic lupus erythematosus. Arthritis Rheum 1982;25:1271–7.
[17] Bombardier C, Gladman DD, Urowitz MB, Caron D, Chang CH. Derivation of the SLEDAI. A disease activity index for lupus patients. The Committee on Prognosis Studies in SLE. Arthritis Rheum 1992;35:630–40.
[18] Pavon EJ, Munoz P, Navarro MD, Raya-Alvarez E, Callejas-Rubio JL, Navarro-Pelayo F, et al. Increased association of CD38 with lipid rafts in T cells from patients with systemic lupus erythematosus and in activated normal T cells. Mol Immunol 2006;43:1029–39.

[19] Zubiaur M, Izquierdo M, Terhorst C, Malavasi F, Sancho J. CD38 ligation results in activation of the Raf-1/mitogen-activated protein kinase and the CD3-zeta/zeta-associated protein-70 signaling pathways in Jurkat T lymphocytes. J Immunol 1997;159:193–205.
[20] Wessel D, Flugge UI. A method for the quantitative recovery of protein in dilute solution in the presence of detergents and lipids. Anal Biochem 1984;138:141–3.
[21] Pavon EJ, Munoz P, Lario A, Longobardo V, Carrascal M, Abian J, et al. Proteomic analysis of plasma from patients with systemic lupus erythematosus: increased presence of haptoglobin alpha2 polypeptide chains over the alpha1 isoforms. Proteomics 2006;6(Suppl. 1):S282–92.
[22] Edgeworth J, Freemont P, Hogg N. Ionomycin-regulated phosphorylation of the myeloid calcium-binding protein p14. Nature 1989;342:189–92.
[23] Zubiaur M, Fernandez O, Ferrero E, Salmeron J, Malissen B, Malavasi F, et al. CD38 is associated with lipid rafts and upon receptor stimulation leads to Akt/protein kinase B and Erk activation in the absence of the CD3-zeta immune receptor tyrosine-based activation motifs. J Biol Chem 2002;277:13–22.
[24] Livak KJ, Schmittgen TD. Analysis of relative gene expression data using real-time quantitative PCR and the 2(−Delta Delta C(T)) Method. Methods 2001;25:402–8.
[25] Rabilloud T, Chevallet M, Luche S, Lelong C. Two-dimensional gel electrophoresis in proteomics: past, present and future. J Proteomics 2010;73:2064–77.
[26] Edgeworth J, Gorman M, Bennett R, Freemont P, Hogg N. Identification of p8,14 as a highly abundant heterodimeric calcium binding protein complex of myeloid cells. J Biol Chem 1991;266:7706–13.
[27] Marenholz I, Lovering RC, Heizmann CW. An update of the S100 nomenclature. Biochim Biophys Acta 2006;1763:1282–3.
[28] Castagnola M, Inzitari R, Fanali C, Iavarone F, Vitali A, Desiderio C, et al. The surprising composition of the salivary proteome of preterm human newborn. Mol Cell Proteomics 2011;10 [M110.003467].
[29] van den Bos C, Roth J, Koch HG, Hartmann M, Sorg C. Phosphorylation of MRP14, an S100 protein expressed during monocytic differentiation, modulates Ca(2+)-dependent translocation from cytoplasm to membranes and cytoskeleton. J Immunol 1996;156:1247–54.
[30] Lominadze G, Rane MJ, Merchant M, Cai J, Ward RA, McLeish KR. Myeloid-related protein-14 is a p38 MAPK substrate in human neutrophils. J Immunol 2005;174:7257–67.
[31] Steinberg TH, Agnew BJ, Gee KR, Leung WY, Goodman T, Schulenberg B, et al. Global quantitative phosphoprotein analysis using Multiplexed Proteomics technology. Proteomics 2003;3:1128–44.
[32] Vogl T, Ludwig S, Goebeler M, Strey A, Thorey IS, Reichelt R, et al. MRP8 and MRP14 control microtubule reorganization during transendothelial migration of phagocytes. Blood 2004;104:4260–8.
[33] Bou G, Villasis-Keever A, Paya CV. Detection of JNK and p38 activation by flow cytometry analysis. Anal Biochem 2003;317:147–55.
[34] Denny MF, Yalavarthi S, Zhao W, Thacker SG, Anderson M, Sandy AR, et al. A distinct subset of proinflammatory neutrophils isolated from patients with systemic lupus erythematosus induces vascular damage and synthesizes type I IFNs. J Immunol 2010;184:3284–97.
[35] Bennett L, Palucka AK, Arce E, Cantrell V, Borvak J, Banchereau J, et al. Interferon and granulopoiesis signatures in systemic lupus erythematosus blood. J Exp Med 2003;197:711–23.
[36] Thorey IS, Roth J, Regenbogen J, Halle JP, Bittner M, Vogl T, et al. The Ca2+-binding proteins S100A8 and S100A9 are encoded by novel injury-regulated genes. J Biol Chem 2001;276:35818–25.
[37] Sheikh AA, Vimalachandran D, Thompson CC, Jenkins RE, Nedjadi T, Shekouh A, et al. The expression of S100A8 in pancreatic cancer-associated monocytes is associated with the Smad4 status of pancreatic cancer cells. Proteomics 2007;7:1929–40.
[38] Zwadlo G, Bruggen J, Gerhards G, Schlegel R, Sorg C. Two calcium-binding proteins associated with specific stages of myeloid cell differentiation are expressed by subsets of macrophages in inflammatory tissues. Clin Exp Immunol 1988;72:510–5.
[39] Sheng WY, Wang TC. Proteomic analysis of the differential protein expression reveals nuclear GAPDH in activated T lymphocytes. PLoS One 2009;4:e6322.
[40] Simard JC, Girard D, Tessier PA. Induction of neutrophil degranulation by S100A9 via a MAPK-dependent mechanism. J Leukoc Biol 2010;87:905–14.
[41] Verma DS, Spitzer G, Zander AR, Fisher R, McCredie KB, Dicke KA. T lymphocyte and monocyte-macrophage interaction in colony-stimulating activity elaboration in man. Blood 1979;54:1376–83.
[42] Pan H, Luo C, Li R, Qiao A, Zhang L, Mines M, et al. Cyclophilin A is required for CXCR4-mediated nuclear export of heterogeneous nuclear ribonucleoprotein A2, activation and nuclear translocation of ERK1/2, and chemotactic cell migration. J Biol Chem 2008;283:623–37.
[43] Payeli SK, Schiene-Fischer C, Steffel J, Camici GG, Rozenberg I, Luscher TF, et al. Cyclophilin A differentially activates monocytes and endothelial cells: role of purity, activity, and endotoxin contamination in commercial preparations. Atherosclerosis 2008;197:564–71.
[44] Yuan W, Ge H, He B. Pro-inflammatory activities induced by CyPA-EMMPRIN interaction in monocytes. Atherosclerosis 2010;213:415–21.